ORIENTATION EFFECTS ON THE INNER REGION OF DUSTY TORUS OF ACTIVE GALACTIC NUCLEI

Toshihiro Kawaguchi and Masao Mori
Center for Computational Sciences, University of Tsukuba, Tsukuba, Ibaraki 305-8577, Japan; kawaguti@ccs.tsukuba.ac.jp

ABSTRACT

A sublimation process governs the innermost region of the dusty torus of active galactic nuclei. However, the observed inner radius of the torus is systematically smaller than the expected radius by a factor of $\sim 1/3$. We show that the anisotropy of the emission from accretion disks resolves this conflict naturally and quantitatively. An accretion disk emits lesser radiation in the direction closer to its equatorial plane (i.e., to the torus). We find that the anisotropy makes the torus inner region closer to the central black hole and concave. Moreover, the innermost edge of the torus may connect with the outermost edge of the disk continuously. Considering the anisotropic emission of each clump in the torus, we calculate the near-infrared flux variation in response to a UV flash. For an observer at the polar angle $\theta_{\rm obs} = 25°$, the centroid of the time delay is found to be 37% of the delay expected in the case of isotropic illumination, which explains the observed systematic deviation.

Key words: accretion, accretion disks – dust, extinction – galaxies: active – galaxies: structure – infrared: galaxies

1. INTRODUCTION

Active galactic nuclei (AGNs) are powered by gas accretion onto supermassive black holes (BHs) at the center of each galaxy. The central BH and the accretion disk are hidden from our line of sight, in some geometry, by an optically and geometrically thick dusty torus (Antonucci & Miller 1985; Miller & Goodrich 1990). Since the torus potentially plays the role of a gas reservoir for the accretion disk, its nature has long been studied (Pier & Krolik 1992; Efstathiou & Rowan-Robinson 1995; Beckert & Duschl 2004; Schartmann et al. 2008).

A large geometrical thickness of the torus is inferred from the detection of high optical polarization, the sharp-edged ionization cone, the near- and mid-infrared (NIR and MIR) to UV luminosity ratio, and the number ratio between type-1 and type-2 AGNs in the unified AGN scheme (Antonucci 1993; Wilson & Tsvetanov 1994; Lawrence 1991). To sustain the geometrical thickness of the torus, the vertical velocity dispersion must be as large as $\sim 100\,{\rm km\,s^{-1}}$. However, it is impossible to explain such a large velocity dispersion by thermal velocity, since dust grains cannot survive over a sublimation temperature $T_{\rm sub} \sim 1500$ K (Barvainis 1987; Laor & Draine 1993). Therefore, Krolik & Begelman (1988) concluded that numerous dusty clumps, rather than a smooth mixture of gas and dust, with a temperature $\lesssim 1500$ K constitute the torus with a large clump-to-clump velocity dispersion (i.e., dusty clumpy torus). Various models for the clumpy torus have been investigated (Nenkova et al. 2002, 2008; Wada & Norman 2002; Dullemond & van Bemmel 2005; Hönig et al. 2006).

The dusty and clumpy torus absorbs optical/UV radiation from the central accretion disk and re-emits as IR radiation (Telesco et al. 1984; Radovich et al. 1999). The energy balance (of each clump) between heating by incident radiation flux and cooling via blackbody radiation indicates that clumps located closer to the central BH have higher temperature. Clumps at the innermost region of the torus have the highest temperature, with a temperature of $T_{\rm sub}$ at the irradiated surface, and emit NIR radiation as "3 μm bump" (Kobayashi et al. 1993). Barvainis (1987) derived the innermost radius of the torus (dust

sublimation radius, denoted as $R_{\rm sub,0}$ in this study):

$$R_{\rm sub,0} = 0.13 \left(\frac{L_{\rm UV}}{10^{44}\,{\rm erg\,s^{-1}}} \right)^{0.5} \left(\frac{T_{\rm sub}}{1500\,{\rm K}} \right)^{-2.8}$$
$$\times \left(\frac{a}{0.05\,\mu{\rm m}} \right)^{-0.5}\,{\rm pc}, \qquad (1)$$

where $L_{\rm UV}$ and a are UV luminosity and the size of dust grains, respectively. If this estimation is correct, the NIR radiation flux varies with a time lag of some months behind the optical/UV flux variations.

Photometric monitoring observations of type-1 AGNs revealed that NIR emission from AGNs indeed lags behind optical variation by an order of a month (Clavel et al. 1989; Glass 2004; Minezaki et al. 2004). Moreover, the luminosity dependency of the time lag also coincides with the theoretical prediction as $\propto L_{\rm UV}^{0.5}$ (Suganuma et al. 2006; Gaskell et al. 2007 using the data presented by Glass 2004). These agreements between the observational results and the theoretical considerations support the idea that the innermost radius of the torus is controlled by the dust sublimation caused by irradiation from the accretion disk.

Despite the successful agreement of luminosity dependency of the NIR-to-optical time lag, however, a conflict appeared concerning the normalization of the time lag. Namely, the time lag measured and collected by Suganuma et al. (2006) is systematically smaller than the lag predicted from Equation (1) by a factor of $\sim 1/3$ (Kishimoto et al. 2007; Nenkova et al. 2008).

In this Letter, we notice that the estimation of dust sublimation radius (Equation (1)) presumes isotropic emission from the accretion disk. Yet, emission from an optically thick disk is, in principle, anisotropic, which is a fact missing in previous theoretical considerations. There is a systematic difference between the inclination angle at which we observe the disk in type-1 AGNs and the angle at which an aligned torus observes the disk. We show that the effects of the anisotropic illumination flux from the accretion disk resolve the systematic discrepancy between the observations and the theory regarding the NIR-to-optical time lag. In the next section, the anisotropy of the disk
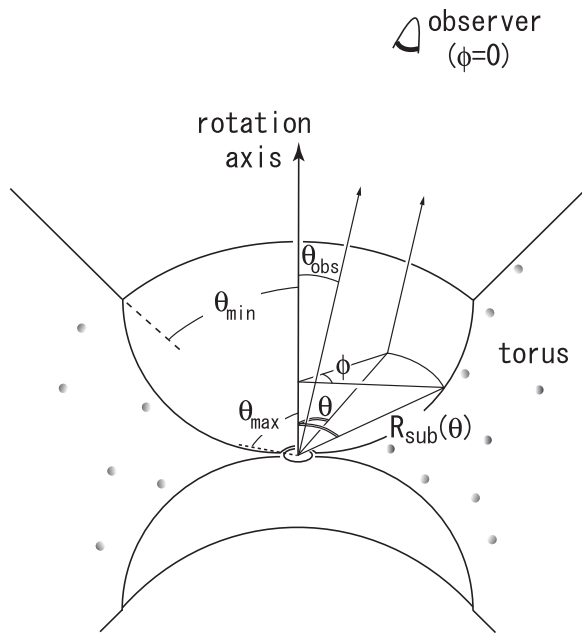
Figure 1. Schematic view of the inner structure of the torus. On the left side of the rotational axis, the definitions of θ_{min} (the torus thickness) and θ_{max} (the disk thickness) are indicated.

Figure 2. Calculated geometry of the innermost region of the dusty torus, where r and z are the cylindrical coordinates. The central BH and the accretion disk in the $z = 0$ plane are located at the origin (not drawn) and are observed with the polar angle $\theta_{obs} = 25°$. We assume alignment between the disk and the torus. In the case of an isotropic illumination, the torus edge has been supposed to stand at $r = R_{sub,0}$. Thick solid line indicates the edge of the torus, with the opening angle of the torus (θ_{min}) assumed to be $45°$. On the right-hand side of the line, clumps contain dust. Dashed line represents $R_{sub}(\theta)$ (Equation (3)). The torus inner edge is located closer to the central BH than in the previous estimations (Equation (1)) and concave/hollow. The innermost region of the torus may connect with the outermost radius of the disk.

emission is introduced. Then, the inner structure of the torus is examined within the framework of clumpy torus models in Section 3. In Section 4, we derive the transfer function for NIR emission of the torus in response to optical/UV flux variation in the disk. Finally, we make a summary and discussion of this study in Section 5.

2. ANISOTROPIC EMISSION OF ACCRETION DISK

Now, let us consider the emission from an optically thick, plain slab (i.e., disk). Radiation flux (F) from a unit surface area of the disk toward a unit solid angle at the polar angle of θ decreases with an increasing θ as follows:

$$F \propto \cos\theta \,(1 + 2\cos\theta). \tag{2}$$

Here, the first term represents the change in the projected surface area, while the latter represents the limb darkening effect for plasma, whose opacity is dominated by electron scattering over absorption (Netzer 1987, and references therein). In other words, an accretion disk emits lesser radiation in the direction closer to its equatorial plane (i.e., larger θ; Laor & Netzer 1989; Sun & Malkan 1989). Consequently, the assumption of isotropic emission from accretion disks (e.g., Equation (1)) obviously overestimates the radiation flux toward the torus. Therefore, it overestimates the inner radius of the torus.

We note that this effect works even if the disk is infinitesimally thin. The fact that the disk has a nonzero thickness brings about another anisotropy of illumination flux, such that the torus is not illuminated below the disk height (near the equatorial plane) at θ larger than a critical angle θ_{max}. Throughout this Letter, we adopt a thin disk (with an aspect ratio of ~0.01), like the standard accretion disk model (Shakura & Sunyaev 1973). The effects of varying disk thickness as a function of accretion rates (Abramowicz et al. 1988; Fukue 2000; Kawaguchi 2003) will be investigated in a forthcoming paper.

The effect of anisotropic emission has already been discussed and referred to as the orientation effect in the context of emission
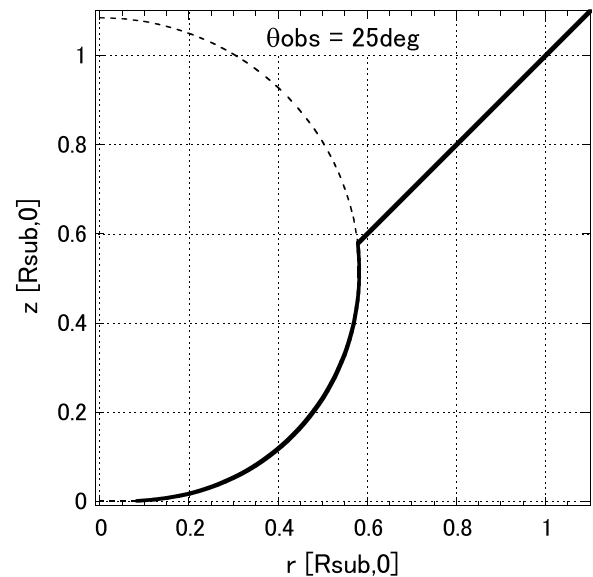
lines, such as the Baldwin effect (Netzer 1985; Francis 1993; Bottorff et al. 1997). However, consequences of this effect upon the torus have not been examined so far. Hereafter, we will explore how this effect influences the torus structure.

3. INNER STRUCTURE OF DUSTY TORUS

We determine the inner edge of the torus so that the temperature of a clump (at the irradiated surface) equals the sublimation temperature at the edge. As mentioned above, radiation flux from the accretion disk varies with the polar angle θ. Thus, the sublimation radius of the torus is also a function of θ, which is indicated by $R_{sub}(\theta)$ in this study (Figure 1). Namely, $R_{sub}(\theta)$ is the distance between the torus edge and the central BH for various θ. To avoid confusion, we express the sublimation radius estimated under the isotropic emission assumption (i.e., Equation (1)), in contrast, as $R_{sub,0}$.

Adopting the anisotropic illumination given in Equation (2), we obtain

$$R_{sub}(\theta) = R_{sub,0} \left[\frac{\cos\theta(1 + 2\cos\theta)}{\cos\theta_{obs}(1 + 2\cos\theta_{obs})} \right]^{0.5}. \tag{3}$$

Here, θ_{obs} is the polar angle toward the observer seen from the central accretion disk, and $\theta_{obs} = 25°$ is assumed throughout this study. Although various grain sizes result in the sublimation process occurring over a transition zone rather than a single distance (Nenkova et al. 2008), we employ a sharp boundary for simplicity.

Figure 2 shows the calculated structure of the innermost region of the torus. The central BH and the accretion disk on the $z = 0$ plane are located at the origin of the coordinate axes (not drawn). If the torus is indeed a reservoir of gas for the disk,

angular momenta of the infalling gas will align these axes. Thus, we assume alignment between the disk and the torus. In the case of an isotropic emission from the disk, the torus edge has been supposed to stand at $r = R_{\mathrm{sub},0}$. A thick solid line indicates the edge of the torus, with the opening angle of the torus ($\theta_{\min}$) assumed to be 45° and the maximum θ of the torus ($\theta_{\max}$) set to 89° (i.e., thin disk approximation mentioned in the previous section). On the right-hand side of the line, the temperatures of clumps are below the dust sublimation temperature. Dashed line represents $R_{\mathrm{sub}}(\theta)$ (Equation (3)) and is drawn as a guide for various $\theta_{\min}$. It turns out that (1) the torus inner edge is located closer to the central BH than suggested by previous estimations (Equation (1)) and that (2) the structure of the edge is concave/hollow. These are the results of weaker illumination flux toward larger θ. Namely, dust can survive closer to the central BH at larger θ.

Moreover, (3) $R_{\mathrm{sub}}(\theta)$ decreases down to $0.1 \times R_{\mathrm{sub},0}$ at $\theta = 88°.5$. This radius coincides with the outermost radius of AGN accretion disks, which is determined by the onset of radial self-gravity of the disk (see Kawaguchi et al. 2004). Little is known about the region outside the outermost radius of the disk (e.g., Collin 2001), such as what happens in the 1 dex gap between the disk outermost radius and the torus innermost radius ($R_{\mathrm{sub},0}$). Our result indicates that there is no gap between the torus and the disk (Emmering et al. 1992; Elitzur & Shlosman 2006).

4. TRANSFER FUNCTION

Although interferometric NIR observations have been made for nearby Seyfert galaxies, only the visibility data, rather than images, are achieved because of the poor u–v coverage (e.g., Kishimoto et al. 2009). Even with the next generation telescope such as Thirty Meter Telescope having 0″.01 spatial resolution at NIR, the innermost radius of the torus discussed above cannot be spatially resolved. Thus, observations of time variability will continue to be powerful tools to explore the innermost structure of the torus in the coming decade. In this section, we calculate the time variation of NIR emission in response to a δ-function-like variation of the irradiation optical/UV flux (the transfer function).

Transfer functions $\Psi(t)$ for various geometries of the re-emitting region have long been studied, mainly in the context of the broad emission line region of AGNs (e.g., Netzer 1990). For instance, a ring produces a double-horned $\Psi(t)$, while a thin (or thick) shell gives a rectangle (or trapezoid). Time variation of the reprocessed radiation (NIR in this study) is a convolution of the illumination flux variation with $\Psi(t)$. The measured time lag corresponds to the centroid of $\Psi(t)$. Below, we calculate $\Psi(t)$ and its centroid in order to compare them with the observational results.

It turned out that it took ∼1 year for the inner region of the dusty torus to adjust to the varying illumination flux (Koshida et al. 2009; Pott et al. 2010). We hereafter regard the inner structure of the torus as time independent in the timescale of NIR-to-optical time lag (∼months).

4.1. Calculation Method

To calculate $\Psi(t)$ for the clumpy torus, we discuss the following three items: (1) the optical path, (2) NIR emissivity of the torus inner region, and (3) anisotropic emission of each clump. In this Letter, we ignore the response from the torus edge at $\theta > \frac{\pi}{2}$, assuming torus self-occultation (absorption of NIR

emission from a clump by other clumps in the line of sight). Although we do not go further, this assumption can be tested in principle via the profile of broad emission lines and its time variation (e.g., Peterson 2001).

First, (1) the optical path difference is written as

$$R_{\mathrm{sub}}(\theta)[1 - \{\cos\theta_{\mathrm{obs}}\cos\theta + \sin\theta_{\mathrm{obs}}\sin\theta\cos\phi\}], \quad (4)$$

where ϕ is the azimuthal angle and defined so that $\phi = 0$ for the observer (Figure 1). The concave shape of the inner region of the torus reduces the optical path difference. Clumps at a distance slightly larger than $R_{\mathrm{sub}}(\theta)$ with a slightly lower temperature than the sublimation temperature will somehow emit NIR radiation. Moreover, clumps at a distance slightly smaller than $R_{\mathrm{sub}}(\theta)$, in the middle of the dust destruction process but with some of their dust grains still surviving, will also emit NIR radiation. These effects will smear out the resultant NIR response $\Psi(t)$. Since these effects are unlikely to change the centroid of $\Psi(t)$ drastically, we here ignore them and consider only optical paths that hit the inner edge of the torus.

Next, (2) we discuss the emissivity of the torus inner region as a function of θ. Since $R_{\mathrm{sub}}(\theta)$ varies with θ, the distance dependency of the NIR emissivity must be determined. Following the calculations of three-dimensional radiative transfer (e.g., Hönig et al. 2006; Schartmann et al. 2008), we assume that (2a) the clump size increases and (2b) the clump number density decreases when the clump-to-BH distance increases, as follows.

Closer to the BH, the tidal force is stronger, thus only smaller clumps are likely to survive there. Therefore, we assume that the clump size is in proportion to the distance between the clump and the central BH. Then, the apparent angular size (observed from the BH) of the clumps at the torus inner edge, which are emitting NIR radiation, is independent of θ. (Farther clumps receiving direct emission from the disk as well are not of interest in this study, because they emit MIR rather than NIR.)

Little is known about the number density of clumps. We assume that the number of clumps at the torus edge per unit solid angle ($d\Omega$) is independent of θ. Namely, the same number of NIR-emitting clumps is contained per $d\Omega$ for various θ. To summarize the two factors, the emissivity of NIR flux per $d\Omega$ is assumed to be proportional to $R_{\mathrm{sub}}(\theta)^2$.

Last, (3) the anisotropy of NIR emission from each clump is considered. To calculate NIR flux, we must care about how extent the illuminated surface of a clump is seen by the observer (Nenkova et al. 2002). Hönig et al. (2006) mentioned that this effect resembles the phases of the moon. Let us suppose that an observer looks at a clump with an angle ξ, where $\xi = 0$ means a face-on view of the illuminated surface (the angle denoted as ϕ in the paper by Hönig et al.). In the case of the moon phase, the anisotropy coefficient (the fraction of the illuminated surface seen by the observer) is $(1+\cos\xi)/2$. However, incident photons can somehow penetrate gaseous clumps, heating up the limb of each clump. Then, the anisotropy is weakened compared with the above estimation for the solid (moon). We adopt the following anisotropic coefficient for the waning effect:

$$\min\left[1, \left(\frac{1+\cos\xi}{2} + 0.1\right)\right]. \quad (5)$$

This coefficient is chosen so as to reproduce the Monte Carlo calculations by Hönig et al. (2006) for a single clump observed from three different ξ. We also try other descriptions for the anisotropy under the condition that each description reproduces the Monte Carlo results, obtaining little difference in the resultant $\Psi(t)$.
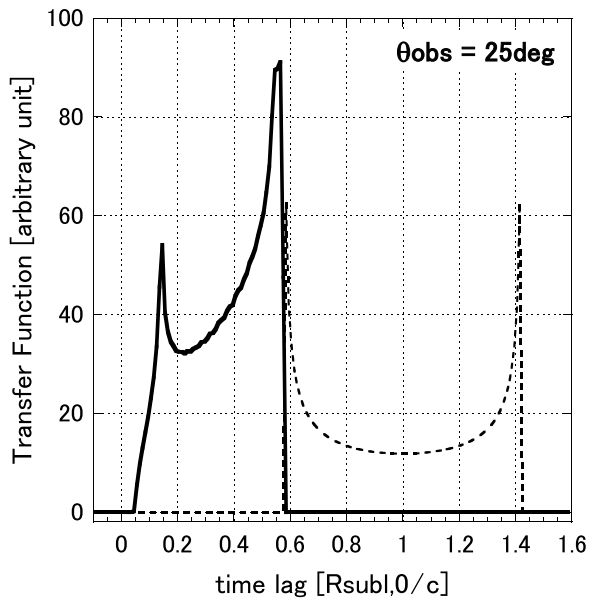
Figure 3. Resultant transfer function for the torus we consider (solid line; NIR response to a δ-function-like variation of illumination flux). Dashed line is the transfer function for a ring with radius $R_{sub,0}$ and $\theta_{obs} = 25°$. In the case of the anisotropic disk emission, the torus responds approximately three times faster than the ring does (the centroid of the transfer function is $0.37\ R_{sub,0}/c$).

4.2. Result

Figure 3 presents the resultant transfer function of the torus for $\theta_{obs} = 25°$ (solid line), calculated by integrating θ (from θ_{min} to θ_{max}) and ϕ (0 to π). The portion at $\phi \sim 0$ produces the left horn, which is a faster (due to a shorter optical path difference, Equation (4)) and weaker (due to the waning effect, Section 4.1) response than the opposite area at $\phi \sim \pi$ (right horn). The dashed line is the transfer function for a ring with radius $R_{sub,0}$ observed from $\theta_{obs} = 25°$ and is drawn for an example of transfer functions in the case of isotropic illumination flux. The ring responds to the illumination flux at around $R_{sub,0}/c$ (where c is the speed of the light) after the δ-function-like variation in the illumination flux at zero time lag. (It is just a coincidence that the ring starts to respond exactly when the torus ends with the current parameter sets.)

On the other hand, the torus we consider shows a faster response and narrower width of the transfer function. These results are due to the fact that the torus inner region we consider is (1) closer to the central BH than $R_{sub,0}$ and (2) concave. The centroid of the time delay of the transfer function is found to be $0.37\ R_{sub,0}/c$, which solves the puzzle of the systematic deviation of a factor of $\sim 1/3$ between the observational results and the theoretical considerations (under the assumption of isotropic emission).

5. SUMMARY AND DISCUSSION

The dusty clumpy torus surrounds the accretion disk and BH in AGNs. Various observations have revealed that the dust sublimation process governs the innermost region of the torus. However, there was a systematic deviation between the observational results and the theory regarding the inner radius of the torus.

In this study, we have shown that the anisotropy of the emission from accretion disks resolves this conflict naturally and quantitatively. Namely, the angle at which we observe the disk in type-1 AGNs is systematically closer to a pole-on view than the angle at which an aligned torus observes the disk. An accretion disk emits lesser radiation in the direction closer to its equatorial plane (larger θ). We have found that the anisotropy makes the torus inner region closer to the central BH and concave. Furthermore, the innermost edge of the torus may connect with the outermost edge of the accretion disk continuously.

Considering the anisotropic emission of each clump, we have calculated the NIR flux variation of the torus in response to a UV flash. A rapid response to the illumination flux is realized, due to the small inner radius and concave shape of the torus. For an observer at $\theta_{obs} = 25°$, the centroid of the time delay is found to be 37% of the delay expected in the case of isotropic illumination.

Other than the orientation effect examined in this study, large grain size (see Equation (1)) and/or extinction between the torus and the accretion disk (i.e., in the broad emission line region) are possible concepts to reduce the inner radius of the torus (Laor & Draine 1993; Maiolino et al. 2001; Gaskell et al. 2007).

Anisotropy is an inevitable feature of the emission from optically thick disks. Even if a BH object (seen in nearly face-on geometry) looks very luminous around the Eddington luminosity, the flux in the directions close to the equatorial plane is not necessarily huge to prevent gas infall. This effect (along with the disk self-occultation) enables gas supply to luminous BH objects. Actually, the observed data do not support the concept of Eddington-limited accretion (Collin & Kawaguchi 2004).

Future studies will examine misalignments between the torus and the disk, and different θ_{obs} (for type 1.5, 1.8, etc., objects), θ_{min} (for objects with a thick/thin torus), and θ_{max} (for thick disks with super-Eddington accretion rates). For instance, some narrow-line Seyfert 1 galaxies and narrow-line QSOs prohibit weak NIR emission (Rodríguez-Ardila & Mazzalay 2006; Kawaguchi et al. 2004; Jiang et al. 2010; however, see Hao et al. 2010). Small θ_{max} due to the disk self-occultation with super-Eddington accretion rates (Fukue 2000) can be a reason for the weakness.

REFERENCES

Abramowicz, M. A., Czerny, B., Lasota, J. P., & Szuszkiewicz, E. 1988, ApJ, 332, 646
Antonucci, R. 1993, ARA&A, 31, 473
Antonucci, R. R. J., & Miller, J. S. 1985, ApJ, 297, 621
Barvainis, R. 1987, ApJ, 320, 537
Beckert, T., & Duschl, W. J. 2004, A&A, 426, 445
Bottorff, M., Korista, K. T., Shlosman, I., & Blandford, R. D. 1997, ApJ, 479, 200
Clavel, J., Wamsteker, W., & Glass, I. S. 1989, ApJ, 337, 236
Collin, S. 2001, in Advanced Lectures on the Starburst–AGN Connection, ed. I. Aretxaga, D. Kunth, & R. Mu'jica (Singapore: World Scientific), 167
Collin, S., & Kawaguchi, T. 2004, A&A, 426, 797
Dullemond, C. P., & van Bemmel, I. M. 2005, A&A, 436, 47
Efstathiou, A., & Rowan-Robinson, M. 1995, MNRAS, 273, 649
Elitzur, M., & Shlosman, I. 2006, ApJ, 648, L101
Emmering, R. T., Blandford, R. D., & Shlosman, I. 1992, ApJ, 385, 460
Francis, P. J. 1993, ApJ, 405, 119
Fukue, J. 2000, PASJ, 52, 829
Gaskell, C. M., Klimek, E. S., & Nazarova, L. S. 2007, arXiv:0711.1025

Glass, I. S. 2004, MNRAS, 350, 1049
Hao, H., et al. 2010, ApJ, 724, L59
Hönig, S. F., Beckert, T., Ohnaka, K., & Weigelt, G. 2006, A&A, 452, 459
Jiang, L., et al. 2010, Nature, 464, 380
Kawaguchi, T. 2003, ApJ, 593, 69
Kawaguchi, T., Pierens, A., & Huré, J.-M. 2004, A&A, 415, 47
Kishimoto, M., Hönig, S. F., Antonucci, R., Kotani, T., Barvainis, R., Tristram, K. R. W., & Weigelt, G. 2009, A&A, 507, L57
Kishimoto, M., Hönig, S. F., Beckert, T., & Weigelt, G. 2007, A&A, 476, 713
Kobayashi, Y., Sato, S., Yamashita, T., Shiba, H., & Takami, H. 1993, ApJ, 404, 94
Koshida, S., et al. 2009, ApJ, 700, L109
Krolik, J. H., & Begelman, M. C. 1988, ApJ, 329, 702
Laor, A., & Draine, B. T. 1993, ApJ, 402, 441
Laor, A., & Netzer, H. 1989, MNRAS, 238, 897
Lawrence, A. 1991, MNRAS, 252, 586
Maiolino, R., Marconi, A., & Oliva, E. 2001, A&A, 365, 37
Miller, J. S., & Goodrich, R. W. 1990, ApJ, 355, 456
Minezaki, T., Yoshii, Y., Kobayashi, Y., Enya, K., Suganuma, M., Tomita, H., Aoki, T., & Peterson, B. A. 2004, ApJ, 600, L35
Nenkova, M., Ivezić, Ž., & Elitzur, M. 2002, ApJ, 570, L9

Nenkova, M., Sirocky, M. M., Nikutta, R., Ivezić, Ž., & Elitzur, M. 2008, ApJ, 685, 160
Netzer, H. 1985, MNRAS, 216, 63
Netzer, H. 1987, MNRAS, 225, 55
Netzer, H. 1990, in Active Galactic Nuclei, ed. R. D. Blandford, H. Netzer, & L. Woltjer (Berlin: Springer), 57
Peterson, B. M. 2001, in Advanced Lectures on the Starburst–AGN Connection, ed. I. Aretxaga, D. Kunth, & R. Mu'jica (Singapore: World Scientific), 3
Pier, E. A., & Krolik, J. H. 1992, ApJ, 401, 99
Pott, J.-U., Malkan, M. A., Elitzur, M., Ghez, A. M., Herbst, T. M., Schödel, R., & Woillez, J. 2010, ApJ, 715, 736
Radovich, M., Klaas, U., Acosta-Pulido, J., & Lemke, D. 1999, A&A, 348, 705
Rodríguez-Ardila, A., & Mazzalay, X. 2006, MNRAS, 367, L57
Schartmann, M., Meisenheimer, K., Camenzind, M., Wolf, S., Tristram, K. R. W., & Henning, T. 2008, A&A, 482, 67
Shakura, N. I., & Sunyaev, R. A. 1973, A&A, 24, 337
Suganuma, M., et al. 2006, ApJ, 639, 46
Sun, W.-H., & Malkan, M. A. 1989, ApJ, 346, 68
Telesco, C. M., Becklin, E. E., Wynn-Williams, C. G., & Harper, D. A. 1984, ApJ, 282, 427
Wada, K., & Norman, C. A. 2002, ApJ, 566, L21
Wilson, A. S., & Tsvetanov, Z. I. 1994, AJ, 107, 1227